JGR Atmospheres

RESEARCH ARTICLE
10.1029/2021JD036095

Dynamical Impacts of Stratospheric QBO on the Global Circulation up to the Lower Thermosphere

A. V. Koval[1,2], N. M. Gavrilov[1], A. I. Pogoreltsev[1,2], and K. K. Kandieva[3]

[1]Saint-Petersburg State University, Saint-Petersburg, Russia, [2]Russian State Hydrometeorological University, Saint-Petersburg, Russia, [3]Institute for Meteorology, Leipzig University, Leipzig, Germany

Key Points:

- In the thermosphere, weakening in residual circulation occurs during the westerly QBO, accompanying by an increase in the temperature
- The sensitivity of the wave-induced eddy circulation to changes in the QBO phase is higher than that of the residual circulation
- Cooling of the polar winter stratosphere during westerly QBO is made by the weakening of planetary wave activity

Correspondence to:

A. V. Koval,
a.v.koval@spbu.ru

Citation:

Koval, A. V., Gavrilov, N. M., Pogoreltsev, A. I., & Kandieva, K. K. (2022). Dynamical impacts of stratospheric QBO on the global circulation up to the lower thermosphere. *Journal of Geophysical Research: Atmospheres*, *127*, e2021JD036095. https://doi.org/10.1029/2021JD036095

Received 25 OCT 2021
Accepted 1 FEB 2022

Author Contributions:

Conceptualization: A. V. Koval
Formal analysis: A. I. Pogoreltsev
Funding acquisition: A. V. Koval
Investigation: A. V. Koval, A. I. Pogoreltsev
Methodology: A. V. Koval, A. I. Pogoreltsev
Resources: A. V. Koval
Software: N. M. Gavrilov, K. K. Kandieva
Supervision: A. V. Koval
Validation: N. M. Gavrilov, K. K. Kandieva
Visualization: A. V. Koval, K. K. Kandieva
Writing – original draft: A. V. Koval
Writing – review & editing: N. M. Gavrilov, A. I. Pogoreltsev, K. K. Kandieva

Abstract To estimate reaction of the atmospheric circulation in the middle and upper atmosphere to changes in phases of equatorial stratospheric quasi-biennial oscillation (QBO), the three-dimensional nonlinear middle and upper atmosphere model (MUAM) is used. This model allows continuous simulations of atmospheric wave propagation from the ground to the thermosphere (300 km and above). The main atmospheric hydrodynamic fields (wind and temperature), components of residual meridional circulation (RMC), and fluxes of mass are calculated based on ensembles containing 16 pairs of model runs for initial conditions corresponding to easterly and westerly QBO phases. To minimize uncertainties in determination of the QBO phases, an approach based on the usage of empirical orthogonal functions (EOFs) is applied. Statistically significant results are obtained illustrating how changes in the planetary waves (PWs) structures promote the spread of QBO effects to polar latitudes and to the thermosphere, through changes in the Eliassen-Palm (EP) flux and its divergence, or through the formation of an eddy meridional circulation. The main contribution to the cooling of the polar winter stratosphere during the westerly QBO is made by the weakening of wave activity, in particular, the weakening of the vertical EP flux, which leads to a weakening of the poleward heat flux. The sensitivity of the wave-induced eddy circulation to changes in the QBO phase is higher than that of the RMC, demonstrating that PWs propagating from the lower troposphere are the most important mechanism for the transfer of global circulation disturbances from the equatorial QBO region to polar latitudes.

1. Introduction

One of the important features of the middle atmosphere dynamics is the quasi-biennial oscillation (QBO) of zonal mean flows at stratospheric heights (e.g., Baldwin et al., 2001; Holton & Tan, 1980). This phenomenon is observed at equatorial latitudes: the direction of the zonal wind changes to the opposite with the period varying between 22 and 34 months. The highest zonal wind velocities are observed at altitudes of 20–30 km: about 20 m/s for westerlies and about 30 m/s for easterlies (Baldwin et al., 2001). Although the QBO is a dynamic process occurring in the stratosphere in the vicinity of the equator, its influence in the form of a quasi-2-year periodicity is observed in the composition of the atmosphere and in hydrodynamic fields at other latitudes and altitudes. For instance, Holton and Tan (1980) analyzed the response of the extratropical circulation to the QBO and showed that it is particularly strong during northern winter, where the zonal mean westerly jet is weaker during the easterly QBO phase (eQBO) than that during the westerly QBO phase (wQBO). Garfinkel et al. (2012) concluded that the QBO effect at high latitudes might be related to the induced changes in the thermally balanced subtropical jet and in the associated changes in the refractive index, which restricts the propagation of transient Rossby waves into the subtropics enhancing transient wave activity and the meridional mass circulation. In addition, as it was shown by Cnossen and Lu (2011), QBO interacts with variations caused by the 11-year solar cycle. Gavrilov et al. (2015) studied peculiarities of planetary wave (PW) and orographic gravity wave (OGW) interactions in the middle and upper atmosphere under different QBO phases. They showed that transitions from eQBO to wQBO can cause PW amplitude changes up to ±(30–90)% at middle and high northern latitudes. According to Koval et al. (2018), variations of PW amplitudes may occur due to nonlinear interactions between PW modes and changes in the global circulation under different QBO phases, which produce changes in the refractivity indices and EP fluxes for PW modes. Recently, studies dedicated to the research of the influence of the QBO phases on the transport of greenhouse gases have become especially relevant (Gabriel, 2019). In particular, the numerical simulation was used to reveal the long-term changes in northern midwinter temperature, zonal wind, and residual circulation, that are much stronger during wQBO than during eQBO. Among the other important

studies dedicated to QBO in the middle atmosphere, Chandran and Collins (2014) and Lubis et al. (2016) should be noted, where WACCM model is used, and Fischer et al. (2008) with the model SOCOL.

To date, there are many studies dedicated to the impacts of stratospheric QBOs on the thermosphere and ionosphere. For example, Echer (2007) studied QBO signals in the foF2 frequency oscillations and showed pronounced QBOs in the ionosphere. However, reasons for these oscillations were outside the scope of the study, that is, there remained the questions of the origin of these signals either from the stratospheric QBO or from similar oscillations of solar activity (ionospheric QBO). The structure of the ionospheric QBO from TEC maps was also studied by Tang et al. (2014). They showed that the ionospheric QBO signal only appears during solar maximum which confirmed indirectly the fact that a source of 2-year variations of atmospheric parameters above 100 km might be solar activity. Wang et al. (2018), using the TIE-GCM model and TIMED/SABER data, studied biennial oscillations in ionospheric parameters, such as TEC, foF2 frequency, and so on, as well as migrating tidal components in the lower thermosphere. They showed that biennial variations in the ionosphere are caused by both the ionospheric QBO and the stratospheric QBO. Moreover, the second factor is much weaker than the first. However, as a mechanism for the vertical propagation of the impact of the stratospheric QBO at the lower boundary of the model, only various components of migrating tides at heights of the mesosphere – lower thermosphere (MLT) were used, while, for example, PWs were not considered. The MUAM model used in our study makes it possible to reproduce not only tides, but also stationary PWs, as well as westward and eastward propagating PWs, from the surface, up to 300–400 km. This allows us to study more accurately, in comparison with previous studies, the impact of the stratospheric QBO on the circulation of the thermosphere: changes in the structures of these PWs at different QBO phases in the equatorial stratosphere are transmitted to high altitudes and affect the atmospheric circulation. It should be noted that we concentrate on studying the role of PWs in vertical propagation of stratospheric QBO impacts, which contribute to the thermospheric QBO should be especially noticeable at low solar activity.

The important question of the method for determining the QBO phases remains still open, despite the wide discussion of this topic by the atmospheric community. For instance, what isobaric level data can be used to determine the QBO phase. The simplest way to divide QBO phases on westerly and easterly in earlier papers is so-called single-level index, which implies consideration of the zonal wind direction in the equatorial stratosphere at specific level (e.g., Holton & Tan, 1980; Inoue et al., 2011; Yamashita et al., 2011). However, the level of wind direction determination varies in different studies from 10 to 70 hPa (Baldwin et al., 2001; Scaife et al., 2014). The choice of the level is justified by significant variations in the wind amplitude from phase to phase. The ambiguity in the choice of the level affects the research results. Additional uncertainties produce also asymmetries in the easterly and westerly QBO wind zone descent rates which were first found in NCEP reanalysis data by Huesmann and Hitchman (2001). To diminish these asymmetries, they proposed the usage of equatorial zonal wind shear anomaly index calculated from zonal wind differences at two heights in the stratosphere. To eliminate asymmetries in the easterly and westerly wind zones, Pogoreltsev et al. (2014) proposed calculating differences between monthly mean for each year and climatological zonal wind velocities over the equator at the pressure level 10 hPa. Positive and negative differences correspond to the westerly and easterly QBO phases. Such procedure gave results similar to the mentioned above equatorial zonal wind shear anomaly index.

In this study, we simulate the effects of different QBO phases on atmospheric circulation, using the middle and upper atmosphere model (MUAM). Oscillations of solar activity are not taken into account in the MUAM. This allows us to study pure dynamic effects of the stratospheric QBO at altitudes up to the lower thermosphere to help clarify the question of the contribution of the stratospheric QBO to wave disturbances in the thermosphere. Moreover, this approach allowed us to demonstrate the importance of changes in the PW structures promoting the spread of QBO effects to polar latitudes and to the thermosphere.

To prepare background and initial conditions for the simulation, we use QBO phase determinations based on the decomposition of observed zonal flux variations with empirical orthogonal functions (EOFs). This approach allows taking into account vertical evolutions of QBO phases and more accurate determinating QBO phases for different years.

The study is structured as follows: Section 1 gives a short review on different approaches for QBO phase determinations and their simulations. Section 2 includes brief descriptions of the MUAM model. Section 3 is dedicated to the methodology for studying QBO signals in the equatorial zonal wind based on EOF usage. Changes

in background wind components, temperature, and fluxes of mass simulated with the MUAM are analyzed in Section 4. Modeled QBO responses of the wave-induced eddy circulation components producing respective fluxes of mass are considered in Section 5. Concluding remarks and discussions are presented in the last section.

2. Numerical MUAM Model

To simulate the general atmospheric circulation from the Earth surface up to thermospheric heights under different QBO phases, a three-dimensional nonlinear mechanistic numerical model of the general circulation of the middle and upper atmosphere (MUAM) presented in Pogoreltsev (2007) and Pogoreltsev et al. (2007) is used. It is based on the global circulation model COMMA developed at the University of Cologne, Germany (Ebel et al., 1995). The MUAM uses standard system of primitive equations in spherical coordinates (Gavrilov et al., 2005). The horizontal grid of the model is 5.625° × 5° in longitude and latitude, respectively. The MUAM uses a log-isobaric vertical coordinate $z = -H*ln(p/p_0)$, where p_0 is the surface pressure and H is the pressure scale height. The MUAM involves parameterizations of radiation heating the atmosphere in the ultraviolet and visible spectral bands from 125 to 700 nm and cooling in the 8, 9.6, 14, and 15 mkm infrared bands accounting breakdown of the local thermodynamic equilibrium at high altitudes. EUV heating parameterization is included in the thermosphere. The main parameters calculated by the model include zonal, meridional and vertical wind components, as well as geopotential height and temperature. The MUAM model can reproduce stationary PWs and atmospheric normal modes (NMs; Pogoreltsev et al., 2014). Low-boundary SPW amplitudes are calculated from the geopotential heights in the lower atmosphere obtained from the UK Met Office stratospheric assimilation data (Swinbank & O'Neill, 1994). As far as MUAM does not reproduce tropospheric weather, tropospheric sources of westward traveling atmospheric NMs are set with additional terms in the heat balance equation of the model, which consist of sets of time-dependent sinusoidal components with periods and latitudinal structures (Hough functions) equivalent to the NMs with zonal wavenumbers $m = 1$ and $m = 2$. The spatial resolution of the MUAM grid does not allow resolving mesoscale atmospheric disturbances, such as internal gravity waves (IGWs), therefore, taking them into account requires the implementation of parameterizations in the model. The MUAM includes a parameterization of thermal and dynamical effects produced by a spectrum of non-orographic IGWs (Gavrilov, 1997) and of mountain waves (Gavrilov & Koval, 2013). Different QBO phases are set in the MUAM using the approach described in the next section.

The important advantage of the MUAM over most analogs is the capability of reproducing global resonance properties of the atmosphere (normal atmospheric modes; Pogoreltsev, 2007). This is important feature that model must meet for an adequate modeling of stratospheric vacillation cycles (Holton & Mass, 1976) responsible for, for example, SSW onset. In addition, simple mechanistic models with a relatively low resolution are do not require significant processing time, while allowing for rapid calculations, including ensemble runs. The MUAM is able to simulate dynamic processes up to heights of 300–400 km, which allows us to simulate atmospheric circulation under different QBO phases, calculate the structure of the residual meridional circulation (RMC), and estimate the meridional mass fluxes up to thermospheric heights.

To improve the statistical significance of the simulations, two series (ensembles) containing 16 pairs of calculations of the MUAM model are obtained for conditions typical for the eQBO and wQBO. In the MUAM model, the ensembles are formed from separate MUAM simulations corresponding to different phases of the mean wind and PWs vacillations in the middle atmosphere. These phases in MUAM are controlled by changes in the date of switching on diurnal solar heating variations and generation of normal atmospheric modes (Pogoreltsev, 2007). The initial and background conditions for all model calculations are taken to be identical. A detailed description of the features of statistical processing of data from ensembles of simulations is presented in Koval (2019).

The scheme of numerical experiments is as follows. MUAM simulations start from an initial windless atmosphere with the climatological globally averaged vertical temperature profile. During the first 30 model days, GW parameterizations in the model are not included and geopotential heights at the lower boundary do not change. Then, the longitudinal geopotential variations (stationary PWs) are specified. Within the first 0–120 days, the MUAM uses daily averaged heating rates. Pogoreltsev (2007) showed that the described procedure allows the model to reach steady-state regime at the end of this time interval. After a day between 120 and 135, daily variations of heating are included and the NM sources are switched on. Starting from the 330th model day, seasonal changes in the zenith angle of the Sun are launched, and days 330–390 correspond to January–February. A

detailed description of the processes taken into account in the current version of the MUAM and the scheme of a numerical experiment can be found in Koval et al. (2021).

3. Determination of the QBO Phases

There are three ways to reproduce the QBO in the general circulation models. Fully interactive high-resolution models can simulate QBOs internally, by using the intrinsic variability of meteorological fields. Another way is to parameterize the missing momentum fluxes driving the QBO. Relatively low-resolution models, including mechanistic models such as MUAM, use the relaxation (nudging) of the modeled zonally averaged zonal wind fields toward observations. However, the advantage of the last models is their relative simplicity and speed of operation, which makes it possible, without sacrificing quality, to perform operational calculations, including statistical processing of ensembles of solutions. Nowadays, there is a program that combines interactive models to compare their ability to reproduce the QBO (Butchart et al., 2018). As it was stated above, the MUAM is not able to reproduce self-consistently stratospheric QBO (unlike major SSW events; Koval et al., 2021), hence the simulations require specifying background and initial hydrodynamic fields for years with different QBO phases.

To minimize the ambiguities in determining the phases of the stratospheric QBO and to take into account vertical evolution of the QBO phases, we use a method proposed by Fraedrich et al. (1993) and Wallace et al. (1993), based on the decomposition of the equatorial zonal flow oscillation using EOFs. This decomposition is basically similar to Fourier analysis, however, instead of using sinusoids, this approach involves basis functions determined from the analyzed fields. This allows detecting larger-scale spatio-temporal patterns that are not necessarily presented by waves. Such method was previously used by various authors, for example, Dunkerton (2017), Gray et al. (2018), and M. B. Andrews et al. (2019). EOF analysis is more objective compared to classic single-level QBO index (e.g., Holton & Tan, 1980; Yamashita et al., 2011) as far as it allows studying vertical evolutions of wind changes at specific altitude ranges. Moreover, due to the maintaining orthogonality in time and space, the EOFs give optimal decompositions of raw data (Wallace et al., 1993).

For the study of the QBO signal in the zonal wind field, data of the Japanese 55-year reanalysis JRA-55 (Kobayashi et al., 2015) is used. Anomalies of the zonal wind are considered relative to the values averaged over years 1958–2019. At each of nine isobaric levels (70, 50, 30, 20, 10, 7, 5, 3, and 1 hPa), between the latitudes of 30°S and 30°N, zonal wind fields are decomposed into series according to the EOF method and the first two main components (Q_1 and Q_2) are analyzed, which are shown in Figures 1a and 1b. The seasonal cycle was subtracted. The first and second EOFs, describe 41% and 37.3% (total 78.3%) of the zonal wind variance. The EOF approach thus allows reducing the amount of data with relatively low loss of information, which is consistent with previous studies (e.g., Fraedrich et al., 1993). In this case, the first two EOFs are enough for describing evolutions of QBO amplitudes and phases.

The analysis of Q_1 vertical structure (red line in Figure 1c) shows a negative correlation between variations of the zonal wind on the pressure surfaces of 20 and 70 hPa (altitudes ∼27 and ∼19 km, respectively). A negative correlation at 7 and 30 hPa is also seen for Q_2 (green line in Figure 1c). Sharp changes in Q_1 at 20 and 70 hPa coincide with changes in the wind direction according to Q_2. As shown below in Figure 2, the amplitude of zonal wind fluctuations is maximum at 20 hPa. Based on these results, we determine QBO phase at 20 hPa, considering Q_1 as the main mode, and Q_2 as the alternating one.

Taking account of the first two EOFs, we investigate OBO vertical structures evolution. In Figure 1d, the horizontal axis shows Q_1 values, and the vertical axis corresponds to the respective Q_2 values for each month from the year 1958–2019 according to JRA-55. Dividing this space into sectors shown in Figure 1d, eight structures corresponding to different phases of stratospheric QBO are selected. Figure 2 shows latitude-height cross-sections of zonal wind anomalies in years 1958–2019, corresponding to eight QBO phases shown in Figure 1d. Considering the anomalies of the mean zonal wind at isobaric surface of 20 hPa, eight types of QBO are distinguished. Observing the plots of Figure 2, one can see a "descent" of the maximum fluctuations of the zonal wind from the stratosphere to the troposphere. At fixed 20 mb pressure level, phases 3 and 4 in Figure 2 correspond to the maximum eastward wind, while phases 7 and 8 are near the maximum of westward wind. Thus, the years corresponding to 2 and 3 phases are attributed to the westerly QBO, while 6 and 7 phases are attributed to the easterly QBO. Analysis of the frequency of occurrence of all QBO phases for the month of January shows that for the entire period from 1958 to 2019 (61 months), for 15 months, there is the wQBO and for 16 months there is eQBO.

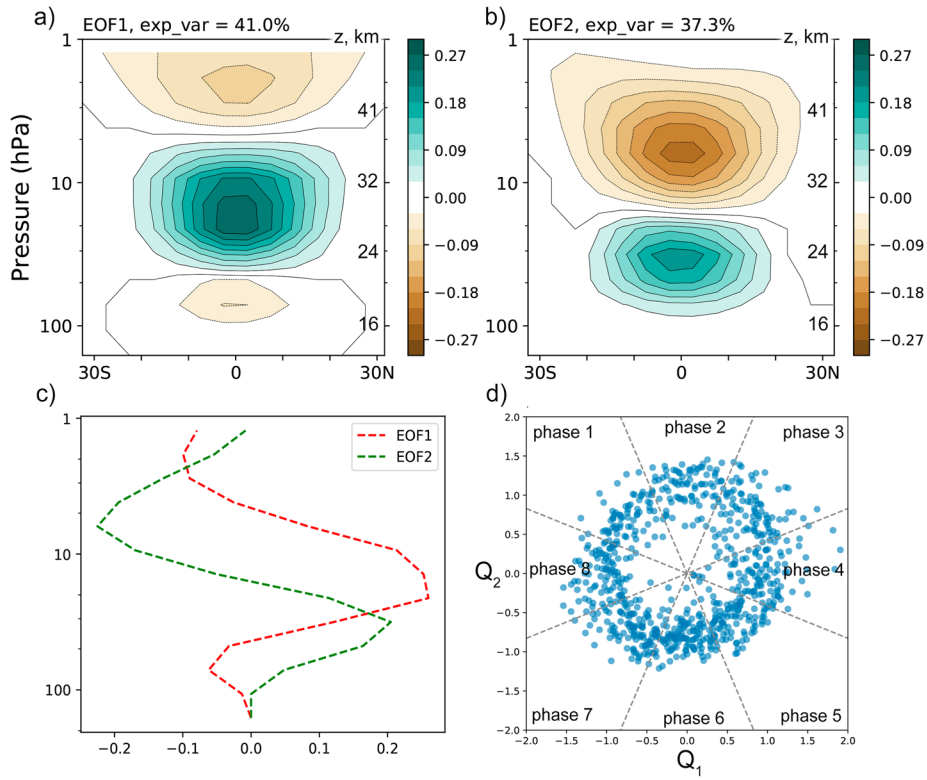

Figure 1. Altitude-latitudinal cross-sections of the EOFs of the zonal wind field Q_1 (a) and Q_2 (b); vertical profiles of Q_1 and Q_2 at the equator (c); scatter diagram of Q_1 and Q_2 (d).

The described above procedure allows us to select two sets containing 10 years with the typical westerly (1983, 1985, 1993, 1995, 1997, 1999, 2002, 2004, 2008, and 2013) and easterly (1987, 1989, 1996, 1998, 2000, 2003, 2005, 2007, 2010, and 2012) QBO phases and calculate average zonal-mean distributions of zonal wind and temperature for both QBO phases.

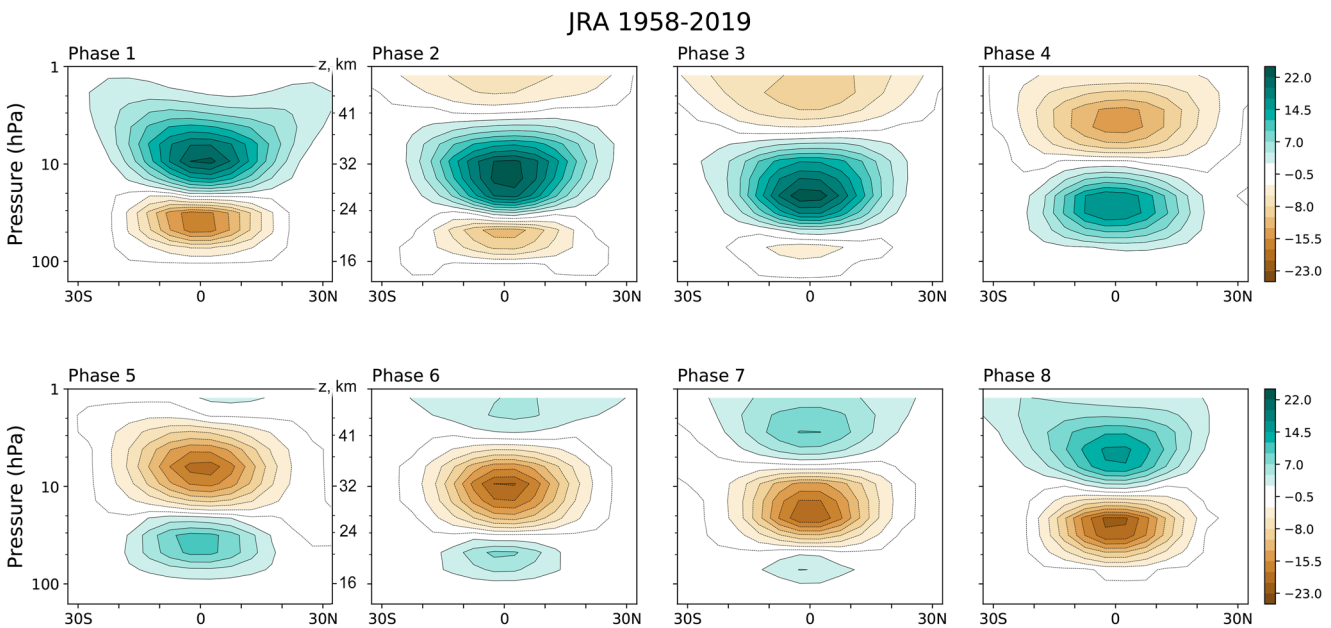

Figure 2. Vertical cross-sections of the mean zonal wind (m/s) corresponding to different QBO phases.

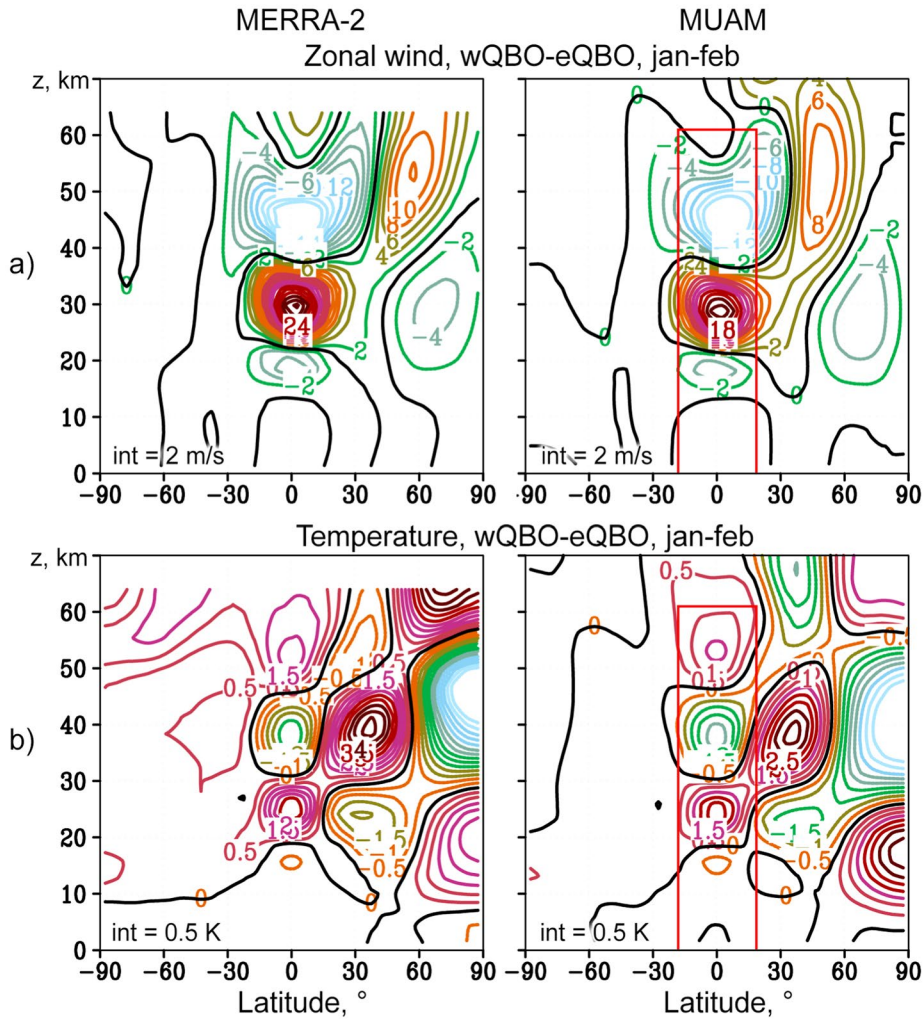

Figure 3. Zonal-mean zonal wind (a) and temperature (b) anomalies due to QBO phase change, calculated based on MERRA-2 reanalysis data (left plots) and MUAM ensemble simulations (right plots) for January–February. Red boxes in the right plots show nudging areas.

3.1. QBO Accounting in the MUAM

To reproduce QBO in the MUAM model, Pogoreltsev et al. (2014) proposed to use additional terms in the momentum equation for zonal wind velocity, which are proportional to differences between calculated and observed zonal mean winds at latitudes from 17.5°S to 17.5°N and altitudes 0–60 km, as it was shown in Equation 4 by Pogoreltsev et al. (2007). The proportionality constant is a value related to the characteristic relaxation time (~5 days) of the calculated hydrodynamic fields to the observed one. The observed zonal mean fields are obtained using the MERRA-2 stratospheric assimilation data (Gelaro et al., 2017) and averaged over the indicated years.

Using the described approach for specifying the QBO phases in the MUAM, simulations of the general atmospheric circulation for January–February were carried out. To increase the statistical significance of the simulations, the mean "climatological" values of hydrodynamic parameters were obtained without taking into account the interannual variability, for both QBO phases. For this purpose, ensembles of 16 model runs were calculated.

Figure 3 shows the averaged over January–February anomalies of the zonal wind (a) and temperature (b) due to the change in the QBO phase, according to the MERRA-2 reanalysis data and according to the ensemble simulations with the MUAM. There is a general similarity in the main trends of the QBO influence: eastward (westward) wind anomalies in the layers of 20–40 (15–20 and 40–55) km in the equatorial region, weakening and warming

of the polar vortex in the lower stratosphere, as well as strengthening of westerlies in the mid-latitude upper stratosphere and mesosphere. According to the classical theory of "thermal wind" (e.g., Gill, 1982), the thermal component of the zonal wind is proportional to the meridional temperature gradient. This effect is observed in the northern stratosphere (between 20 and 30 km), where the cooling of the subtropical region and the warming of the circumpolar region are accompanied by a weakening of the zonal wind. Our simulations are consistent also with the results of Rao et al. (2019) who investigated the structure of stratospheric circulation based on 10 reanalyses of meteorological information and on numerical simulations. White et al. (2015) analyzed changes in zonal wind and temperature by processing ERA-Interim data, from the European Center for Medium-Range Weather Forecasts (ECMWF) for the period of 1979–2012. They considered the vertical dipole structure of temperature anomalies in the stratosphere and related changes in the velocity of vertical flows, induced by the QBO in this region.

4. Zonal-Mean Circulation up to Thermospheric Heights

Figure 4 reveals the latitude-altitude distributions of the zonal wind (a) and temperature (b), averaged for January-February, according to the data of empirical atmospheric models (left), modeling data for the easterly QBO (in the center), and the increments of these values due to QBO phase change from westerly to easterly. The left panels use data from model HWM-14 (Drob et al., 2015) for zonal wind and from NRLMSIS 2.0 (Emmert et al., 2020) for temperature. These models are significantly superior in data quality to previous versions, in particular, compared to the previous version of NRLMSISE-00, numerous edits have been made to NRLMSIS 2.0, including the extension of atomic oxygen down to 50 km and usage of geopotential height as the vertical coordinate, which made it possible to simplify the expressions for the density profiles. New extensive assimilation of the lower and middle atmosphere temperature and gas species according to satellite data was involved. The authors of the model (Emmert et al., 2020) showed that the changes introduced contributed to an increase in the time efficiency of the model and an increase in the correlation of hydrodynamic fields with observational data. Comparison of the left and middle panels in Figures 4a and 4b shows that the MUAM satisfactorily reproduces the considered fields up to the heights of the thermosphere. However, performing the point-by-point comparison is impossible, as far as in the middle plot, distributions for the eQBO are shown, while HWM14 and NRLMSIS do not allow to differentiate QBO phases. In addition, in the real atmosphere, QBO effects overlap with other global oscillations, such as El Nino–Southern Oscillation (ENSO), North Atlantic oscillation (NAO), Madden-Julian oscillation (MJO), and others, which are not set in the model.

To interpret the changes in circulation and identify possible PW contributions to its structure, the meridional and vertical components of the Eliassen-Palm flux (EP flux) $F_m = (F_m^{(\varphi)}, F_m^{(z)})$ were calculated according to the formulas (D. G. Andrews et al., 1987):

$$F_m^{(\varphi)} = \cos\varphi \left(\overline{u}_z \frac{\overline{v'\theta'}}{\overline{\theta}_z} - \overline{u'v'} \right) \tag{1}$$

$$F_m^{(z)} = \cos\varphi \left(\left(f - \frac{\left(\overline{u}\cos\varphi\right)_\varphi}{a\cos\varphi} \right) \frac{\overline{v'\theta'}}{\overline{\theta}_z} - \overline{w'u'} \right). \tag{2}$$

Here, overbars denote the zonal-mean values, primes mark deviations of the values from the zonal-mean values; lower indices mark corresponding partial derivatives; u, v, and w are zonal, meridional, and vertical velocities; $\theta = Texp\left(\frac{g}{Cp}\int_0^h \frac{\mu}{T} dh\right)$ is the potential temperature; h is the geopotential height; C_p is the heat capacity at constant pressure; φ is the latitude; f is the Coriolis parameter. The divergence of the EP flux was also calculated using the formula by D. G. Andrews et al. (1987):

$$\nabla \bullet F_m = \frac{1}{a\cos\varphi} \frac{\partial}{\partial\varphi} \left(F_m^{(\varphi)} cos\varphi \right) + \frac{\partial F_m^{(z)}}{\partial z} \tag{3}$$

In the middle and right plots of Figure 4a, the contours indicate the EP flux divergence, calculated with Equation 3. According to the PW theory, the divergence of the EP flux is accompanied by the acceleration of the eastward zonal mean flow due to PW influences, while the negative divergence, that is, convergence, corresponds to accelerations directed to the west. Thus, in the high-latitude winter stratosphere, the wave action contributes to the acceleration of the eastward wind, while its deceleration is observed at the middle latitudes. However,

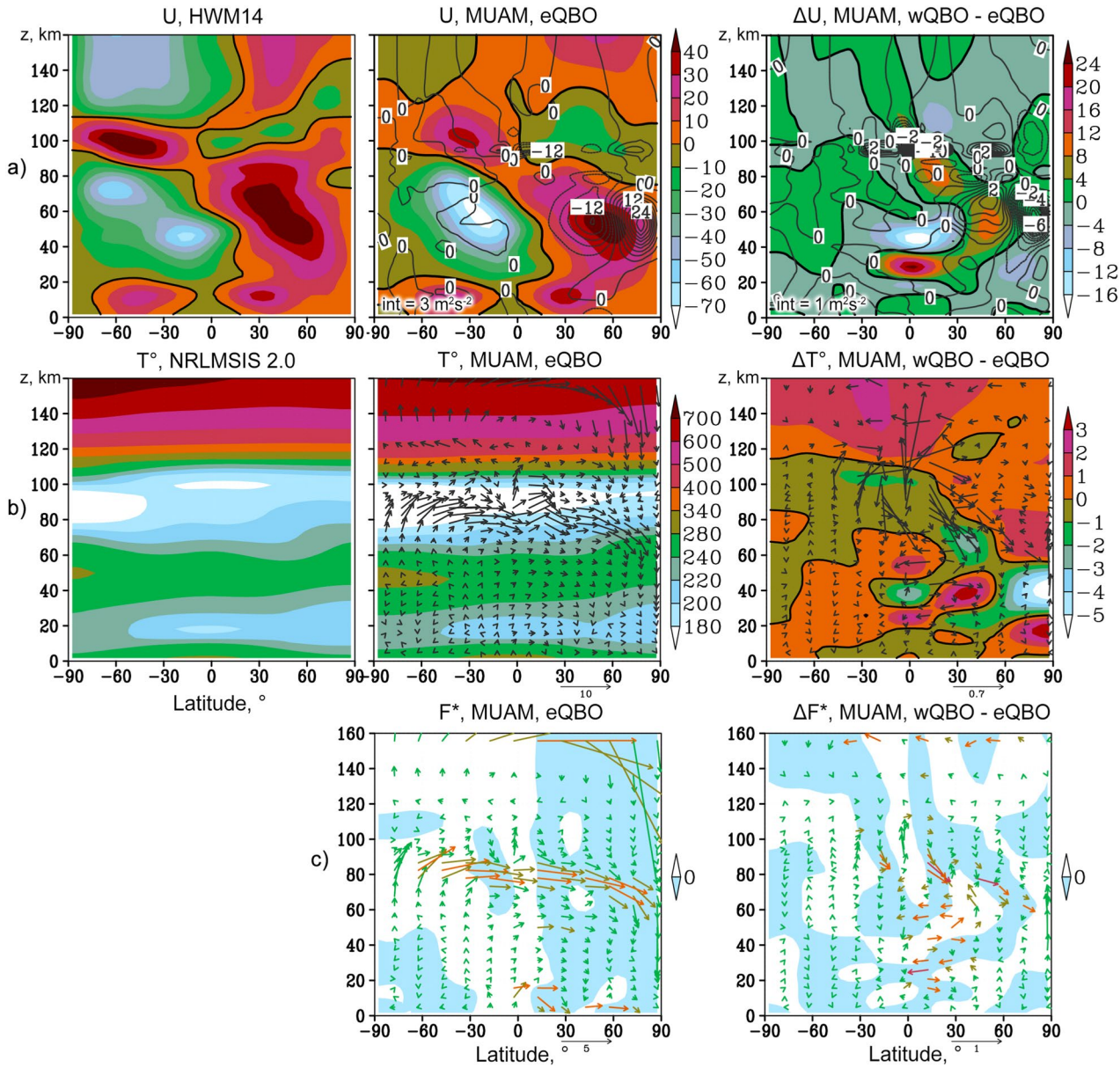

Figure 4. Winter altitude-latitude distributions (shaded) of the zonal-mean wind in m/s (a), temperature in K (b) and residual meridional fluxes of mass in $e^{h/8}$ kg/m^2/s (c) according to HWM14 and NRLMSISE-00 models (left), MUAM simulations (middle) and (wQBO-eQBO) differences of respective quantities (right). Contours in the panels (a) reveal EP-flux divergence (middle) and its difference (right) in 10^{-2} m^2/s^2/day. Arrows in panels (b) and (c) show, respectively, composite RMC flows and meridional mass fluxes (middle) and their (wQBO-eQBO) differences (right) with vertical components multiplied by 200.

the formation of jet streams in the middle atmosphere is also influenced by other factors, the main of which is the inhomogeneity of the heating of the atmosphere, leading to the formation of temperature gradients in the latitudinal direction. These mechanisms are perfectly distinguishable if we consider the distributions of the increments of the zonal wind and temperature due to changes in the QBO phase, presented in the right panels in Figures 4a and 4b, respectively. For example, the acceleration of the stratospheric zonal wind in the latitude range of 30°–60°N is accompanied by a simultaneous increase in the EP flux divergence and by a decrease in temperature, which contributes to a decrease in the meridional temperature gradient. Thus, it can be concluded that the acceleration of the zonal wind in the specified region during wQBO is simultaneously caused by both wave and thermal effects. A similar conclusion can be made when considering the region closer to the pole, where, on the contrary, there is a deceleration of the zonal flow, a decrease in the EP flux divergence, and an increase in the meridional thermal gradient.

A statistical significance of the obtained increments in wind and temperature was calculated based on standard formulas with the approach described by Koval (2019). At each grid node of the latitude-altitude distribution, the paired Student's *t*-test is applied for 32 values (16 pairs of model runs * 2 months). The calculation gives 95% statistical significance of nonzero differences in Figure 4 for values of $|\Delta U| > 2$ m/s and $|\Delta T| > 1$ K. This is true for most regions in the right panels of Figures 4a and 4b, except for the intervals just along zero contours.

In the middle and right panels of Figure 4b, arrows show the composite mean RMC and its changes. For better visibility, the vertical component is multiplied by 200. The meridional and vertical components of the residual mean meridional circulation in terms of the transformed Eulerian mean (TEM) are obtained from the ensembles of hydrodynamic fields simulated with the MUAM using standard formulas (e.g., Koval et al., 2021):

$$\bar{v}^* = \bar{v} - \frac{1}{\partial\bar{\theta}/\partial z}\left(-\frac{\overline{v'\theta'}}{H} + \frac{\partial\overline{v'\theta'}}{\partial z} - \frac{\overline{v'\theta'}}{\partial\bar{\theta}/\partial z}\frac{\partial^2\bar{\theta}}{\partial z^2}\right), \tag{4}$$

$$\bar{w}^* = \bar{w} + \frac{1}{a\cos\varphi}\frac{1}{\partial\bar{\theta}/\partial z}\left(-\sin\varphi\overline{v'\theta'} + \cos\varphi\left(\frac{\partial\overline{v'\theta'}}{\partial\varphi} - \frac{\overline{v'\theta'}}{\partial\bar{\theta}/\partial z}\frac{\partial^2\bar{\theta}}{\partial z\partial\varphi}\right)\right), \tag{5}$$

where a is the radius of the Earth, $H = RT/\mu g$ is the pressure scale height, R is the universal gas constant, T is the temperature, μ is the molar mass of the atmosphere, and g is the gravity acceleration. In the above-mentioned formulas, for the correct calculation of the RMC in the thermosphere, realistic height profiles of μ and C_p above the homosphere, as well as changes in g with height, are involved.

At altitudes above the stratopause, in the middle panel of Figure 4b, there is a significant flow from the summer to the winter hemisphere, with a pronounced maximum in the MLT region and an increase in the thermosphere. When considering the increments of the RMC between wQBO and eQBO in the right panel of Figure 4b, the relationship between temperature changes and vertical residual velocity is clearly visible at low and middle latitudes. The upward or downward movement of air parcels is accompanied by their adiabatic cooling/heating, which contributes to a decrease/increase in temperature in the corresponding layer of the atmosphere. In the stratosphere, temperature changes under different QBO phases correspond to the distributions calculated based on the MERRA-2 meteorological information reanalysis database (see the left panel of Figure 3b).

In the latitudinal belt of 10°–30°N, at MLT heights, an increase in the northward and downward residual circulation is clearly distinguishable in Figure 4, which contributes to the enhancement of the eastward mean flow during wQBO. At heights of the thermosphere in the right panel of Figure 4b, the RMC vectors are directed mainly in the opposite direction relative to the general structure of the RMC in the middle panel of Figure 4b, which indicates a weakening of the RMC in this layer during wQBO. This effect is accompanied by an increase in the temperature of the thermosphere, the main reason for which is a slowdown in the meridional transport of air masses from the warmer summer thermosphere.

In the high-latitude winter stratosphere (between 20 and 50 km), a decrease in temperature is observed, which is primarily caused by a weakening of the upward vertical component of the EP flux shown in the right panel of Figure 5. This is explained by the fact that according to Equation 2 for the vertical component of the EP flux (see also D. G. Andrews et al., 1987), the upward flux corresponds to the wave heat flux directed to the north. Accordingly, the weakening of this flux in the high-latitude middle atmosphere during the westerly QBO phase contributes to the "shortage" of thermal energy in this area. Also, an important contribution to the cooling of this region is made by the weakening of the descending branch of the RMC, shown in the right Figure 4b.

4.1. Meridional Flux of Mass

The application of the RMC concept provides diagnostics of the wave effect on the mean flow, and also makes it possible to calculate the processes of transport of gas species in the meridional plane (D. G. Andrews et al., 1987). For a deeper study of the mechanisms of transport of atmospheric species, the residual meridional mass fluxes in the meridional and vertical directions, F^*_y and F^*_z, respectively, were calculated by multiplying the meridional and vertical RMC components by the atmospheric density at the corresponding nodes of the model grid:

$$F_i^* = \rho\bar{v}_i^*, \quad \rho = \frac{p_0}{RT}\exp\left(-\int_0^h \frac{g\mu dh}{RT}\right), \tag{6}$$

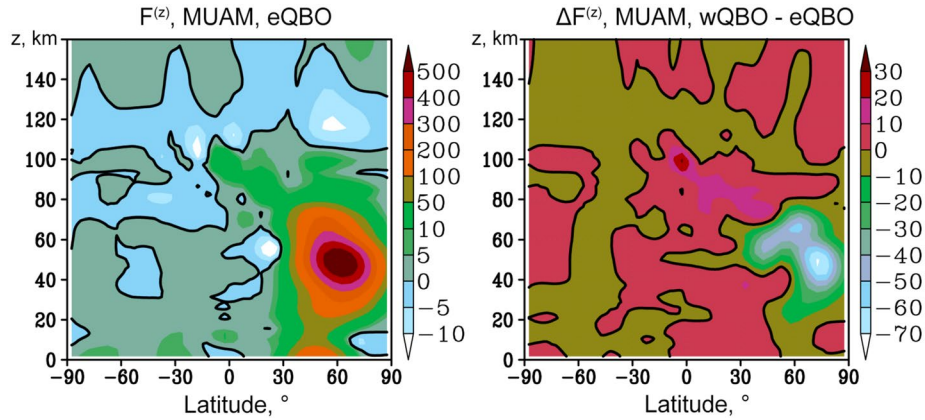

Figure 5. Vertical component of the EP-flux (left) for the eQBO and its increments due to change from wQBO to eQBO in 10^4 m^3/s^2.

where $i = y, z$ correspond to meridional and vertical components, respectively; p_0 is the pressure at the ground (at $h = 0$). The residual velocities indicate the transport of potential temperature. In this case, we assume that air mass and other tracers are transported similarly to that of potential temperature, that is, along the same trajectories and with the same velocities.

Figure 5c shows the latitude-altitude distributions of F^*_y и F^*_z and their increments due to the change in the QBO phase. These values quasi-exponentially decrease with height due to a decrease in atmospheric density, therefore, for clarity purposes, they are multiplied by $e^{h/8}$ and the vertical component is additionally multiplied by 200. The distributions of mass fluxes generally correspond to the direction of meridional circulation shown in the middle panel of Figure 4b. A deep branch of the Brewer-Dobson circulation is observed in the stratosphere (Butchart, 2014) with a tropical upwelling shifted to summer high latitudes and extratropical downwelling in the middle and high latitudes of both hemispheres. Downward fluxes are highlighted in blue.

Above 60 km, there is a global mass transfer from the summer to winter hemisphere with the maximum of the interhemispheric transfer located in the MLT region, as well as an increase in the flux in the thermosphere. An interesting feature of the distribution of the increments of mass fluxes in the right Figure 4c is a general weakening of the interhemispheric mass transfer in the stratosphere, in the latitude range 0°–30°N, coinciding with the areas of the zonal wind amplification, and the increase in the transfer in the areas of weakening of the zonal wind. There is also a significant weakening of the descending mass fluxes in the polar winter stratosphere, corresponding to the cooling of this region during wQBO. At the same time, above 60 km, warming is observed at high Northern latitudes associated with increased horizontal advection and the transfer of warmer masses from lower latitudes.

The observed add-ons to the fluxes of mass due to change in QBO phase can significantly influence thermal regime and transport of conservative tracers in the middle and high atmosphere. Study of the global transport of mass is important not only due to its influence on thermal regime of the middle and upper atmosphere, but also for estimating respective transport of conservative aerosol and gas species, responsible for the climate changes, for instance, ozone. However, at altitudes above 30 km, interactive models of atmospheric chemistry and dynamics are required for more detailed description of atmospheric ozone. At lower altitudes, ozone fluxes may follow the RMC mass fluxes considered in this section.

5. Wave-Induced Eddy Circulation

To study the so-called wave-induced eddy circulation, differences between the residual and Eulerian zonal-mean velocity components $v_{eddy} = \bar{v}^* - \bar{v}$; $w_{eddy} = \bar{w}^* - \bar{w}$ are obtained. These eddy components contribute to non-zonal motions produced mainly by atmospheric PWs (D. G. Andrews et al., 1987).

Figure 6 depicts the meridional (a) and vertical (b) components of the eddy circulation, as well as their increments caused by the change in the QBO phase. In Figure 6b, on the left, one can see that the main contribution of the

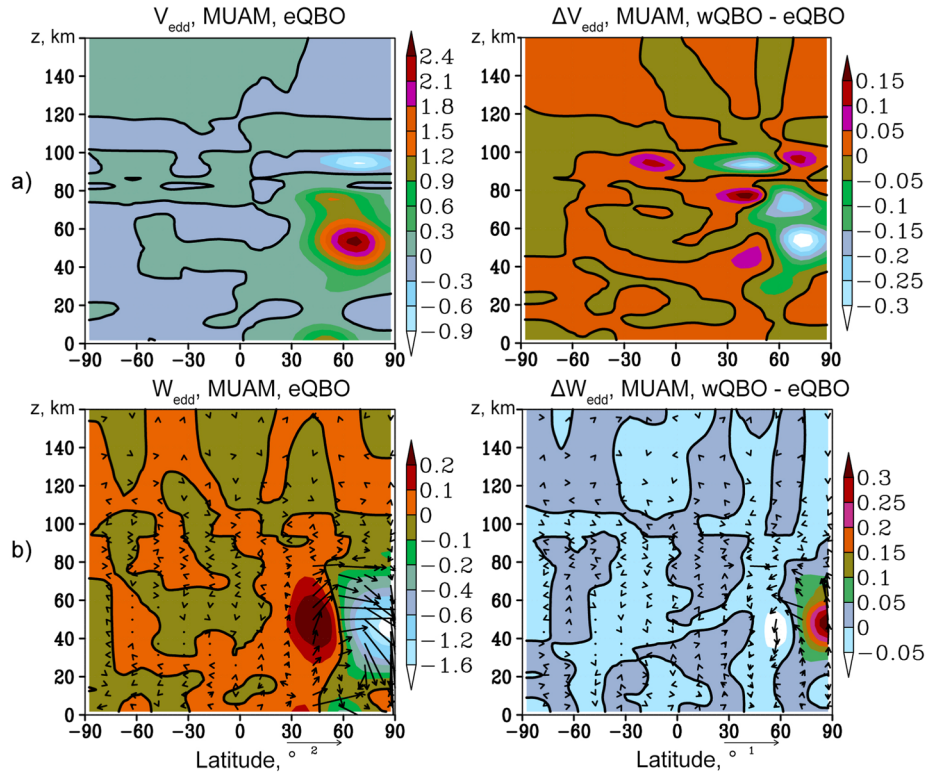

Figure 6. Meridional in m/s (a) and vertical in 200 m/s (b) components of the wave-induced eddy circulation velocity. Arrows show corresponding schematic eddy mass fluxes. ($F_{y,eddy}$, $e^{h/8}$; $F_{z,eddy}$, $200*e^{h/8}$ kg/m^2/s).

eddy component is made in the winter stratosphere, in the regions of the predominant PW distribution (e.g., Dickinson, 1968; Gavrilov et al., 2015). The contribution of the eddy circulation is expressed in the weakening of the downdrafts in the mid-latitude stratosphere and their intensification in the high-latitude region. In this case, together with the northward-directed meridional component shown in the left Figure 6a, this wave-induced contribution creates an additional circulation cell of opposite direction relative to the mean Eulerian circulation (see, e.g., Koval et al., 2019). In the areas of maximum eddy components in the right Figures 6a and 6b, a reversal of the meridional circulation can be observed. This is consistent with the conventional theory (Butchart, 2014). Earlier, Garny et al. (2014) discussed similar results showing that wave-induced eddy components may cause recirculation of air in the stratosphere, which leads to decelerations of the Eulerian zonal-mean circulation. Above 100 km, the considered eddy circulation gradually decays due to the sharply increasing vertical temperature gradients in these layers, which are included in Equations 1 and 2 as the denominator.

In the right Figures 6a and 6b, one can see that during wQBO, a general weakening of the eddy circulation occurs poleward from 40° to 50°N. The main reason for this effect is the attenuation of the wave action on the mean flow, accompanied by a weakening of the EP flux, shown in Figure 5 on the right, which contributes to the generation of eddy circulation. At lower northern latitudes, the opposite effect can be observed—an increase in the meridional component at altitudes below 90 km.

5.1. Zonal-Mean Eddy Mass Fluxes

Arrows in Figure 7b represent schematic vectors of zonal-mean eddy mass fluxes $F_{y,eddy}$ and $F_{z,eddy}$ calculated using Equation 6 after replacing $\bar{v}_i^*$ by eddy velocity components $\bar{v}_{eddy}$, $\bar{w}_{eddy}$. For the sake of illustration, $F_{y,eddy}$ and $F_{z,eddy}$ are multiplied by $e^{h/8}$ and $200*e^{h/8}$, respectively. The arrows visualize all features of eddy circulation at different QBO phases. Contributions of the wave-induced eddy circulation lead in general to the formation of additional cell of mass fluxes transport in the northern stratosphere, which is clearly seen in the left Figure 6b. Similar to eddy circulation, eddy mass fluxes gradually attenuate above 100 km.

The relative changes in eddy mass fluxes at different QBO phases can reach 20% in the winter stratosphere and hence, are important for the transport of mass and conservative tracers in the middle atmosphere. Moreover, if we compare Figures 4c and 6b, changes in the eddy circulation prevail frequently over changes in the residual circulation, that is, wave processes make the most significant contributions to the change in the structure of the RMC in the winter stratosphere at different phases of the QBO. This leads to a very important conclusion that PWs propagating from the lower troposphere are among the most important mechanisms for the transfer of global circulation disturbances from the equatorial stratosphere, where the QBO are originated, to polar regions.

6. Conclusion

Using ensembles (series) of the MUAM model runs, numerical simulation of the atmospheric general circulation, as well as the RMC and associated meridional fluxes of mass at altitudes up to the thermosphere at different QBO phases for January–February, has been performed. The sensitivity of circulation to changes in the QBO phase has been investigated. Compared to previous similar studies, we managed to study the dynamic influence of the stratospheric QBO up to the heights of the thermosphere in its pure form, without superimposing other effects, such as, for instance, oscillations of solar activity (ionospheric QBO).

For determining the QBO phases, the approach based on EOFs is used. This technique allows the simplest and most effective way to minimize the ambiguity in determining the QBO phases, considering not only the change in the direction of the zonal wind at a certain altitude, but also the general time evolution of the zonal wind structure in the entire stratosphere. Using the described methodology, years with the easterly and westerly QBO phases have been selected, and the initial conditions for MUAM simulations in the middle and upper atmosphere have been selected.

It is shown that the simulated atmospheric circulation structure at different QBO phases corresponds to the data of the reanalysis of meteorological information for the same set of years that is used for the MUAM initialization.

The main results can be structured as follows:

1. The greatest contribution to the changes in the zonal wind speed observed in the Northern Hemisphere is made by changes in the PW structures, due to changes in the EP flux divergence. Also, an important source of changes in zonal circulation are meridional temperature gradients. The relative changes in the zonal wind speed in the winter middle atmosphere can reach 15%.
2. Temperature changes at different QBO phases are closely related to changes in the meridional circulation structure. At low and middle latitudes, temperature changes are connected with the vertical residual velocity. Upward or downward movements of air parcels are accompanied by their adiabatic cooling/heating, which contributes to a decrease/increase in temperature in corresponding layers of the atmosphere. Contributions to the cooling of the polar winter stratosphere during the wQBO could be made by the weakening of wave activity, in particular, the weakening of the vertical EP flux, which leads to a weakening of the heat fluxes directed toward the pole.
3. In the thermosphere, the RMC weakening occurs during the westerly QBO phase. This effect is accompanied by an increase in the temperature of the thermosphere, the main reason for which is a slowdown of the meridional transport of air masses from the warmer summer thermosphere.
4. An interesting feature of changes in residual mass fluxes due to changes in the QBO phase is a general weakening of interhemispheric mass transfer in the stratosphere at latitudes of 0°–30°N, coinciding with the areas of increased zonal wind, as well as an increase in the transfer in areas of weakening zonal wind.
5. The sensitivity of the wave-induced eddy circulation to changes in the QBO phase is higher than that of the RMC. The reason for this effect is the change in wave activity in the winter stratosphere. This demonstrates a very important conclusion that PWs propagating from the lower troposphere are the most significant mechanism for the transfer of global circulation disturbances from the equatorial region, where the QBO is originated, to the polar regions.

Study of the global transport of mass is important not only due to its influence on thermal and dynamic regime of the middle and upper atmosphere, but also because of their important role in transport of conservative aerosol and gas species, responsible for the climate changes. The described results of studies at heights of the thermosphere

are especially important during the minimum solar activity, when the relative contribution of the impact of wave structures propagating from the lower atmosphere to the oscillations of the upper atmosphere is maximized.

In the future, it would be useful to calculate and analyze PW structures and their dependence on the stratospheric QBO at the heights of the thermosphere, especially the so-called "fast" PWs (high-frequency PWs with periods of up to 5 days and zonal wavenumbers 1–3) that can penetrate directly from the lower atmosphere upwards and have a direct impact on the dynamics and composition of the ionosphere.

Data Availability Statement

All data sets presented in the study can be freely accessed at https://doi.org/10.5281/zenodo.5596370. According to the statement 1296 of the Civil Code of the Russian Federation, all rights on the MUAM code belong to the Russian State Hydrometeorological University (RSHU). To get access to the computer codes and for their usage, a reader should get permission from the RSHU Rector at the address 79, Voronezhskaya street, St. Petersburg, Russia, 192007, phone: 007 (812) 372-50-92. The authors will assist in getting such permission.

Acknowledgments
Numerical simulations of the atmospheric global circulation and PW structures are supported by the Ministry of Science and High Education of the Russian Federation (Agreement 075-15-2021-583). Calculations and analyses of the residual mean circulation and corresponding mass fluxes are supported by the Russian Science Foundation (Grant # 20-77-10006).

References

Andrews, D. G., Holton, J. R., & Leovy, C. B. (1987). *Middle atmosphere dynamics* (pp. 489). Academic Press.

Andrews, M. B., Knight, J. R., Scaife, A. A., Lu, Y., Wu, T., Gray, L. J., et al. (2019). Observed and simulated teleconnections between the stratospheric Quasi-Biennial Oscillation and Northern Hemisphere winter atmospheric circulation. *Journal of Geophysical Research: Atmospheres*, *124*, 1219–1232. https://doi.org/10.1029/2018JD029368

Baldwin, M. P., Gray, L. J., Dunkerton, T. J., Hamilton, K., Haynes, P. H., Randel, W. J., et al. (2001). The quasi-biennial oscillation. *Reviews of Geophysics*, *39*(2), 179–229. https://doi.org/10.1029/1999rg000073

Butchart, N. (2014). The Brewer-Dobson circulation. *Reviews of Geophysics*, *52*, 157–184. https://doi.org/10.1002/2013RG000448

Butchart, N., Anstey, J. A., Hamilton, K., Osprey, S., McLandress, C., Bushell, A. C., et al. (2018). Overview of experiment design and comparison of models participating in phase 1 of the SPARC Quasi-Biennial Oscillation initiative (QBOi) . *Geoscientific Model Development*, *11*, 1009–1032. https://doi.org/10.5194/gmd-11-1009-2018

Chandran, A., & Collins, R. L. (2014). Stratospheric sudden warming effects on winds and temperature in the middle atmosphere at middle and low latitudes: A study using WACCM. *Annals of Geophysics*, *32*, 859–874. https://doi.org/10.5194/angeo-32-859-2014

Cnossen, I., & Lu, H. (2011). The vertical connection of the quasi-biennial oscillation modulated 11 year solar cycle signature in geopotential height and planetary waves during Northern Hemisphere early winter. *Journal of Geophysical Research*, *116*, D13101. https://doi.org/10.1029/2010JD015427

Drob, D. P., Emmert, J. T., Meriwether, J. W., Makela, J. J., Doornbos, E., Conde, M., et al. (2015). An update to the Horizontal Wind Model (HWM): The quiet time thermosphere. *Earth and Space Science*, *2*, 301–319. https://doi.org/10.1002/2014EA000089

Dunkerton, T. J. (2017). Near identical cycles of the Quasi-Biennial Oscillation in the equatorial lower stratosphere. *Journal of Geophysical Research: Atmospheres*, *122*, 8467–8493. https://doi.org/10.1002/2017JD026542

Ebel, A., Berger, U., & Krueger, B. C. (1995). Numerical Simulations with COMMA, a Global Model of the Middle Atmosphere. *SIMPO Newsletter*, *12*, 22–32.

Echer, E. (2007). On the quasi-biennial oscillation (QBO) signal in the foF2 ionospheric parameter. *Journal of Atmospheric and Solar-Terrestrial Physics*, *69*, 621–627. https://doi.org/10.1016/j.jastp.2006.11.001

Emmert, J. T., Drob, D. P., Picone, J. M., Siskind, D. E., Jones, M. Jr., Mlynczak, M. G., et al. (2020). NRLMSIS 2.0: A whole-atmosphere empirical model of temperature and neutral species densities. *Earth and Space Science*, *7*, e2020EA001321. https://doi.org/10.1029/2020EA001321

Fischer, A. M., Schraner, M., Rozanov, E., Kenzelmann, P., Schnadt Poberaj, C., Brunner, D., et al. (2008). Interannual-to-decadal variability of the stratosphere during the 20th century: Ensemble simulations with a chemistry-climate model. *Atmospheric Chemistry and Physics*, *8*, 7755–7777. https://doi.org/10.5194/acp-8-7755-2008

Fraedrich, K., Pawson, S., & Wang, R. (1993). An EOF analysis of the vertical time delay structure of the Quasi-Biennial Oscillation. *Journal of the Atmospheric Sciences*, *50*(20), 3357–3365. https://doi.org/10.1175/1520-0469(1993)050<3357:AEAOTV>2.0.CO;2

Gabriel, A. (2019). Long-term changes in the northern midwinter middle atmosphere in relation to the Quasi-Biennial Oscillation. *Journal of Geophysical Research: Atmospheres*, *124*(13), 914–942. https://doi.org/10.1029/2019JD030679

Garfinkel, C. I., Butler, A. H., Waugh, D. W., Hurwitz, M. M., & Polvani, L. M. (2012). Why might stratospheric sudden warmings occur with similar frequency in El Niño and La Niña winters? *Journal of Geophysical Research*, *117*, D19106. https://doi.org/10.1029/2012jd017777

Garny, H., Birner, T., Bönisch, H., & Bunzel, F. (2014). The effects of mixing on age of air. *Journal of Geophysical Research: Atmospheres*, *119*, 7015–7034. https://doi.org/10.1002/2013JD021417,2014

Gavrilov, N. M. (1997). Parameterization of momentum and energy depositions from gravity waves generated by tropospheric hydrodynamic sources. *Annales Geophysicae*, *15*(12), 1570–1580. https://doi.org/10.1007/s00585-997-1570-4

Gavrilov, N. M., & Koval, A. V. (2013). Parameterization of mesoscale stationary orographic wave forcing for use in numerical models of atmospheric dynamics. *Izvestiya Atmospheric and Oceanic Physics*, *49*(3), 244–251. https://doi.org/10.1134/s0001433813030067

Gavrilov, N. M., Koval, A. V., Pogoreltsev, A. I., & Savenkova, E. N. (2015). Simulating influences of QBO phases and orographic gravity wave forcing on planetary waves in the middle atmosphere. *Earth Planets and Space*, *67*, 86. https://doi.org/10.1186/s40623-015-0259-2

Gavrilov, N. M., Pogoreltsev, A. I., & Jacobi, C. (2005). Numerical modeling of the effect of latitude-inhomogeneous gravity waves on the circulation of the middle atmosphere. *Izvestiya Atmospheric and Oceanic Physics*, *41*(1), 9–18.

Gelaro, R., McCarty, W., Suárez, M. J., Todling, R., Molod, A., Takacs, L., et al. (2017). The modern-era retrospective analysis for research and applications, version 2 (MERRA-2). *Journal of Climate*, *30*(14), 5419–5454. https://doi.org/10.1175/JCLI-D-16-0758.1

Gill, A. E. (1982). *Atmosphere-ocean dynamics* (pp. 662). Academic Press.

Gray, L. J., Anstey, J. A., Kawatani, Y., Lu, H., Osprey, S., & Schenzinger, V. (2018). Surface impacts of the quasi-biennial oscillation. *Atmospheric Chemistry and Physics*, *18*(11), 8227–8247. 10.5194/acp-18-8227-2018

Holton, J. R., & Mass, C. (1976). Stratospheric vacillation cycles. *Journal of the Atmospheric Sciences*, *33*, 2218–2225. https://doi.org/10.1175/1520-0469(1976)033<2218:svc>2.0.co;2

Holton, J. R., & Tan, H. (1980). The influence of the equatorial quasibiennial oscillation on the global circulation at 50 mb. *Journal of the Atmospheric Sciences*, *37*, 2200–2208. https://doi.org/10.1175/1520-0469(1980)037<2200:tioteq>2.0.co;2

Huesmann, A. S., & Hitchman, M. H. (2001). The stratospheric quasi-biennial oscillation in the NCEP reanalyses: Climatological structures. *Journal of Geophysical Research*, *106*(D11), 11859–11874. https://doi.org/10.1029/2001JD900031

Inoue, M., Takahashi, M., & Naoe, H. (2011). Relationship between the stratospheric quasi-biennial oscillation and tropospheric circulation in northern autumn. *Journal of Geophysical Research*, *116*, D24115. https://doi.org/10.1029/2011JD016040

Kobayashi, S., Ota, Y., & Harada, H. (2015). The JRA-55 reanalysis: General specifications and basic characteristics. *Journal of the Meteorological Society of Japan*, *93*, 5–48. https://doi.org/10.2151/jmsj.2015-001

Koval, A. V. (2019). Statistically significant estimates of influence of solar activity on planetary waves in the middle atmosphere of the Northern Hemisphere as derived from MUAM model data. *Solar-Terrestrial Physics*, *5*(4), 53–59. https://doi.org/10.12737/stp-54201907

Koval, A. V., Chen, W., Didenko, K. A., Ermakova, T. S., Gavrilov, N. M., Pogoreltsev, A. I., et al. (2021). Modelling the residual mean meridional circulation at different stages of sudden stratospheric warming events. *Annals of Geophysics*, *39*, 357–368. https://doi.org/10.5194/angeo-39-357-2021

Koval, A. V., Gavrilov, N. M., & Pogoreltsev, A. I. (2019). Sensitivity of meridional mean circulation to the impact of orographic waves at different phases of quasi-biennial oscillations in a numerical model of the middle atmosphere. *Russian Journal of Physical Chemistry B*, *13*(4), 674–680. https://doi.org/10.1134/S1990793119040092

Koval, A. V., Gavrilov, N. M., Pogoreltsev, A. I., & Savenkova, E. N. (2018). Comparisons of planetary wave propagation to the upper atmosphere during stratospheric warming events at different QBO phases. *The Journal of Atmospheric and Solar-Terrestrial Physics*, *171*, 201–209. https://doi.org/10.1016/j.jastp.2017.04.013

Lubis, S. W., Matthes, K., Omrani, N. E., Harnik, N., & Wahl, S. (2016). Influence of the Quasi-Biennial Oscillation and Sea Surface Temperature Variability on Downward Wave Coupling in the Northern Hemisphere. *Journal of the Atmospheric Sciences*, *73*(5), 1943–1965. https://doi.org/10.1175/JAS-D-15-0072.1

Pogoreltsev, A. I. (2007). Generation of normal atmospheric modes by stratospheric vacillations. *Izvestiya - Atmospheric and Oceanic Physics*, *43*(4), 423–435.

Pogoreltsev, A. I., Savenkova, E. N., & Pertsev, N. N. (2014). Sudden stratospheric warmings: The role of normal atmospheric modes. *Geomagnetism and Aeronomy*, *54*(3), 357–372.

Pogoreltsev, A. I., Vlasov, A. A., Fröhlich, K., & Jacobi, C. (2007). Planetary waves in coupling the lower and upper atmosphere. *The Journal of Atmospheric and Solar-Terrestrial Physics*, *69*, 2083–2101. https://doi.org/10.1016/j.jastp.2007.05.014

Rao, J., Yu, Y. Y., Guo, D., Shi, C. H., Chen, D., & Hu, D. Z. (2019). Evaluating the Brewer–Dobson circulation and its responses to ENSO, QBO, and the solar cycle in different reanalyses. *Earth and Planetary Physics*, *3*(2), 166–181. https://doi.org/10.26464/epp2019012

Scaife, A. A., Athanassiadou, M., Andrews, M., Arribas, A., Baldwin, M., Dunstone, N., et al. (2014). Predictability of the quasi-biennial oscillation and its northern winter teleconnection on seasonal to decadal timescales. *Geophysical Research Letters*, *41*(5), 1752–1758.

Swinbank, R., & O'Neill, A. (1994). Stratosphere-troposphere assimilation system. *Monthly Weather Review*, *122*, 686–702.

Tang, W., Xue, X.-H., Lei, J., & Dou, X.-K. (2014). Ionospheric quasi-biennial oscillation in global TEC observations. *Journal of Atmospheric and Solar-Terrestrial Physics*, *107*, 36–41.

Wallace, J. M., Panetta, R. L., & Estberg, J. (1993). Representation of the equatorial stratospheric Quasi-Biennial Oscillation in EOF phase space. *Journal of the Atmospheric Sciences*, *50*(12), 1751–1762. https://doi.org/10.1175/1520-0469

Wang, J. C., Tsai-Lin, R., Chang, L. C., Wuc, Q., Lin, C. C. H., & Yue, J. (2018). Modeling study of the ionospheric responses to the quasi-biennial oscillations of the sun and stratosphere. *Journal of Atmospheric and Solar-Terrestrial Physics*, *171*, 119–130.

White, I. P., Mitchell, N. J., & Phillips, T. (2015). Dynamical response to the QBO in the Northern Winter stratosphere: Signatures in wave forcing and eddy fluxes of potential vorticity. *Journal of the Atmospheric Sciences*, *72*, 4487–4507. https://doi.org/10.1175/JAS-D-14-0358.1

Yamashita, Y., Akiyoshi, H., & Takahashi, M. (2011). Dynamical response in the Northern Hemisphere midlatitude and high#latitude winter to the QBO simulated by CCSR/NIES CCM. *Journal of Geophysical Research*, *116*, D06118. https://doi.org/10.1029/2010JD015016